A Ground Control and Subsidence Study of a Longwall Mine in Southern Illinois

Yoginder P. Chugh, Zhanjing Yu, Paul E. Miller
Department of Mining Engineering
Southern Illinois University
Carbondale, IL 62901

Abstract

This paper presents the results of an ongoing field geotechnical study in a longwall mine in southern Illinois. The study includes both surface and underground instrumentation and monitoring. Surface subsidence monitoring includes vertical and horizontal deformations of sixty-five monuments along and across the study panel, and underground instrumentation includes measurement of changes with face retreat in vertical pressure and horizontal deformation of chain pillars, and roof-floor convergence, roof sag, and floor heave in entries. An attempt is made to correlate the surface and in-mine ground movements. A hyperbolic tangent equation appears to fit changes in pillar deformation, convergence, and surface subsidence data as a function of face position very well. The developed equations may be used by the mining industry to plan additional supports in entries, vacating surface structures, and in planning land use over mined-out areas.

Introduction

Ground mechanics in longwall mining should consider surface and subsurface deformations as well as stresses and displacements in the vicinity of the longwall face as they impact face and mine stability. In the past, most studies (Mark, 1990; Newman, 1989; Peng and Chiang, 1984; Bauer and Hunt, 1982; among others) emphasized either surface deformations or in-mine stability studies. In this research, both surface deformations and in-mine stability studies are being conducted, and its objectives are to study: 1) subsidence characteristics, including time effects; 2) stress and deformation changes in chain pillars as a function of time and face location; 3) roof, pillar and floor deformations in entries as a function of time and face location; and 4) relationships between the surface subsidence and underground strata behavior. Subsidence over chain pillars is of considerable interest to the coal industry in the Illinois Coal Basin, and the long-term goal of this research is to design chain pillars with controlled subsidence movements.

Mine Description and Geology

The mine extracts the Herrin (No.6) coal seam in southern Illinois at an average depth of 650 ft from the surface. A typical lithologic log for a borehole in the area is shown

in Figure 1. The thickness of the coal in this area varies from 100 to 120 in. which includes a 5-to-13-in. shale parting (Blue Band) 18 to 20 in. above the coal bottom. Core-holes near this site indicate an immediate roof of 4.5 to 5.5 ft of black shale with a relatively competent 21 ft thick limestone immediately above. The black shale breaks into small discs quite easily, with occasional pyrite flakes. About 6 to 12 in. of coal is left along the roof in the gate entries to avoid the falls of the immediate roof bed which is typically sensitive to moisture. Roof bolts are anchored into the limestone bed. The immediate floor strata consist of light gray underclay ranging from 2 to 5 ft in thickness, underlain by 10 to 15 ft of hard calcareous shale, with limestone nodules throughout. In this area, the Springfield (No. 5) coal seam is 40 to 50 ft below the No. 6 coal seam. Near the surface, the core-holes show 30 to 50 ft of glacial material underlain by layers of shale, limestone, sandstone, and coal markers to the limestone.

The chain pillars are designed on 120 ft x 60 ft centers, using a three-entry system with 15.5 ft wide entries (Figure 2). The pillars are offset at the crosscuts by approximately 15 ft. The longwall face is 960 ft wide and 7,000 ft long in the east-west direction. Two panels had already been extracted immediately to the north of the study panel, and two more panels immediately to the south of the study panel will be extracted in the future (the layout permitted us to plan the study over the next three years.). The longwall face retreats approximately 30 ft per day toward the east. Dowty two-leg 500-ton shield supports are used on the face. Additional roof supports are used in between crosscuts at the head and tailgate entries on an as-needed-basis using timber sets, crib blocks and truss bolting. Escapeways along the solid coal block are also timbered with sets containing an 8 ft cross beam and two posts 8 in. x 8 in. in cross-section.

The gate and tail entries of the previously mined panels were physically examined to determine the extent and range of the floor heave, pillar settlements, pillar failures and roof failures. Floor heave down the center of the tail entries (6 in. to 18 in.) was visible, but it was not discernible in the headgate entries. The interface between the pillar and the floor was dug at a few locations in tailgate entries which revealed that the coal pillar had punched at least 6 in. into the weak floor. Occasional roof falls were observed along the gate entries. Most pillars were, however, intact, with little rib sloughing, and it was concluded that pillar instrumentation would stand a chance for survival for long-term monitoring.

Instrumentation Layout

The instrumentation chain pillars underground were selected about 720 ft away from the panel's termination point and about 1000 ft away from the retreating longwall. The surface and underground instrumentation layouts are shown in Figures 2 and 3. Surface instrumentation consisted of subsidence monitoring for vertical and horizontal displacements. The underground instrumentation consisted of measuring roof-floor convergence, lateral pillar deformations, pillar loads, roof sag and floor heave. Underground instrumentation began on February 1, 1992, and by February 29, 1992, most of the instrumentation had been completed. At that time, the longwall face was within 310 ft of the nearest underground instrumentation point. A brief discussion of the instrumentation and data gathering is presented here, and a detailed description is given

by Chugh et al. (1992) elsewhere.

Subsidence Instrumentation

Figure 3 illustrates the subsidence monitoring network. Four subsidence monitoring lines consisting of 65 monuments were established. The main monitoring line is along the transverse direction of the panel, and the three fork lines are along the longitudinal direction of the panel. The monuments were located at 60 ft intervals over the center of the panel and at 30 ft intervals near the edges. The distance between monuments along the longitudinal forks was 60 ft. A 7 ft subsidence monitoring point, with a frost-free design, was used in the study. Vertical displacement was measured with Second Order-Class II accuracy level surveying. The requirement for accuracy for such a survey is 8 mm $\sqrt{k}$ where k is the loop distance in km. An autoset level with an optical micrometer (least count 0.0001 m or 0.000328 ft) and two invar leveling rods were utilized for measurement. Horizontal displacement measurements were measured using a steel tape with a resolution of 0.010 ft. The readings were estimated to the nearest 0.005 ft. The distance between two monuments was measured two times and averaged. Vertical displacements of monuments, not undergoing subsidence, fluctuated within 3 mm due to measurement and physical change errors.

Subsidence surveys were conducted at intervals varying from two (2) days to seven (7) days, depending upon expected movements. The baseline data was collected on February 7, 1992, and the subsidence monitoring line was undermined on or about March 16, 1992.

Vibration Wire Stress Meters

Pillar stress changes were measured using the vibrating wire stressmeter (VWS). A total of eight (8) VWSs were installed in the two chain pillars on the headgate of the panel as shown in Figure 3. The VWS holes were drilled horizontally from the rib, and one VWS was installed in each hole at a depth of 15 ft. At the time of the installation, the longwall face was about 550 ft behind the outby row of the VWSs (VWSs 4-1-6-2 as shown in Figure 3). VWS #5 was destroyed when the face passed by, and VWSs #1, #4, and #6 were blocked due to the collapse of the middle entry when the face was located about 400 ft, outbye, of the instrumented pillars. The VWSs were monitored at intervals varying from two (2) to thirty (30) days, depending upon the expected changes. The accuracy of the VWS measurement is about 3.5 psi.

Roof-Floor Convergence Measurement

A convergence station consisted of a "S" hook attached to the head of a roof bolt and an eye bolt anchored 6 in. into the floor. In order to prevent floor monitoring points from being run over by mining machinery, the eye-bolts in the floor were covered with PVC caps. Twenty (20) convergence stations were installed at Site 1 and the location of each station is shown in Figure 3. All the stations were located around the two instrumented pillars, except #11 which was about 200 ft inby. A tape extensometer with the resolution

of 0.005 in. was utilized for convergence measurement.

Horizontal Pillar Deformation

Horizontal pillar deformations were monitored using a MPBX probe. Two MPBX monitoring sets were installed as shown in Figure 3; one 20 ft deep, and the other 5 ft deep from the pillar rib. A MPBX set-up consists basically of three components: borehole C-anchors, a probe guide and an expansion shell anchor. The borehole C-anchor is a polymer cylinder with a magnet set in the anchor body, and a maximum of ten (10) anchors may be installed in one hole. A PVC probe guide tube runs through the anchors, and the position of each magnet relative to a magnet in the surface anchor is measured using the flexible Sonic probe and a readout box. The accuracy of the measurements is expected to be on the order of 0.5 pct. of the length being measured. Differential displacements between any two anchors can be calculated by referring to the surface anchor.

Roof Sag Measurement

Roof sag measures displacement of the roof only in contrast to convergence which measures roof-floor displacement. Two roof sag stations were installed at Site 1 as shown in Figure 3. Roof sag was measured similarly to convergence. Instead of a 6 in. floor anchor, a 5 ft bolt, grouted in competent floor strata, was used. Since the vertical displacement of the weak floor strata is not measured by this station, the measured convergence is primarily roof sag if the displacement of the hard strata below the weak floor is negligible. All underground instrumentation was monitored at intervals varying from two (2) to thirty (30) days, depending upon the expected changes.

Results and Discussion

Subsidence Across the Panel

The progressive vertical subsidence, horizontal strain, slope and curvature profiles across the panel with retreating face are shown in Figures 4 through 7.

1) The maximum subsidence measured is 5.71 ft which represents a subsidence factor of 0.75 (Actual mined height of the seam, as provided by the company, was used in this calculation.). The location of the maximum subsidence is skewed toward the tailgate side because of the influence of the adjacent mined-out panel. The skewness gradually shifts toward the headgate side as the overburden settles (Figure 4). The maximum strain, slope and curvature observed are 0.0188, 0.047 and 3.85/mile, respectively. These values are all above the threshold values from a structural damage point of view (Yu et al., 1988).

2) The angle of draw values on the headgate side (based on 0.01 ft and 0.03 ft of edge vertical subsidence) are about 30.1 deg. and 20.5 deg., respectively.

3) The location of the point of maximum tensile strain and the inflection point are over the mined out area (Figures 5 and 7). The maximum tensile strain on the headgate and tailgate sides are located about 115 ft and 13 ft from the panel edge. The location of the maximum tensile strain matches very well with the location of the cracks observed on the surface by visual inspection. The offset distance, which is the distance of the inflection point from the panel edge, is 164 ft on the headgate side and 55 ft on the tailgate side. The measurements on the tailgate side, however, reflect subsidence due to retreating of the study panel only.

4) The subsidence over the tailgate entries is much larger (19.78 in.) than that over the headgate entries (2.4 in.) as shown in Figure 4. The larger subsidence on the tailgate side may be due to both pillar failure and floor failure. The maximum subsidence, strain, slope and curvature on the tailgate side are, however, much smaller than those on the headgate side (Figures 4 through 7) due to more uniform subsidence, and due to the fact that subsidence monuments on the tailgate side were installed after the longwall face to the north had been mined.

5) Most of the subsidence occurs after the longwall face has passed the surface monitoring points. Only about 5 pct of the total subsidence had occurred when the face was vertically below the surface monitoring line. About 85 pct of the total subsidence had occurred within 10 days when the face retreated about 265 ft (0.4 H) outby of the monitoring line.

Subsidence Along the Panel

The dynamic subsidence profiles for the three longitudinal fork lines were very similar. Therefore, the progressive subsidence, and horizontal strain only along the middle fork are shown in Figures 8 and 9.

1) The lengths of the monitoring forks are not long enough and should be about 450 ft long to observe a complete dynamic subsidence cycle.

2) The locations of the maximum tensile strains for the Middle, South and North fork lines are 75 ft, 105 ft and 105 ft behind the face (in the gob area), respectively. These values are appropriate because at the middle of the panel the overburden has less support from the chain pillar than at the edges and therefore it tends to break more quickly at the panel center than at the side of the panel.

3) The displacements of the inflection points toward the gob is 164 ft for the middle line, 210 ft for the South line and 150 ft for the North line, respectively. These values are similar to those calculated across the panel.

4) In general, the maximum travelling horizontal strain, slope and curvature values for all the forks are less than the static ones (those across the panel). For

example, the maximum values for the traveling horizontal strain, slope and curvature along the middle line are 0.00965, 0.026 and 1.46/mile, which are 51%, 55.3% and 38% of the static values, respectively.

Subsidence as a Functions of Time or Face Position

Normalized measured vertical subsidence, S/Smax as a function of normalized face position (d/H) for a point on the monitoring line in the center of the panel is shown in Figure 10. The above two variables were correlated using a general hyperbolic tangent equation below

$$\frac{S}{S_{max}} = \frac{1}{2}\left(1-\tanh\left(B\frac{A-d}{H}\right)\right) \qquad (1)$$

where A and B are constants. The predicted and measured data are shown in Figure 10 and indicate very good fit between the two. A and B values used are 200 ft and 4.67, respectively. The curve may be subdivided into three phases.

Phase I - It represents small amount of total subsidence (5-10 pct) and subsidence occurs slowly at an approximately linear rate with face retreat.

Phase II- It represents accelerated subsidence rate and most of the subsidence occurs during this phase. Subsidence rate during this phase may also be assumed linear. About 80 pct of the total subsidence occurs during this phase.

Phase III- subsidence rate during this phase decays exponentially as the distance from the face to the monitoring point increases. This represents the residual subsidence and about 5-10 pct of the total subsidence occurs during this phase.

An attempt was also made to fit the data for convergence, and lateral pillar deformations to the generalized equation above. The results of these analysis are presented later in this paper.

Instead of d/H, the equation may be written in terms of any time (t) and time T required to reach maximum subsidence:

$$\frac{S}{S_{max}} = \frac{1}{2}\left(1-\tanh\left(\frac{t-\frac{T}{2}}{C}\right)\right) \qquad (2)$$

where C and T are constants. The above equation was fitted to the data and for T=100 days and C= 6 days, the correlation coefficient for the best-fit line was 0.994. Approximate subsidence rates during Phase I, Phase II, and Phase III are given in Table 1.

Stress Changes in the Chain Pillars

The stress changes along the VWS line 4-1-6-2, which represent the distribution of stress changes in the two pillar in the transverse direction, are shown in Figure 11. It is difficult to determine from the data if and how much of the pillars have yielded, because only two VWSs were installed along the transverse line of each pillar.

The stress changes in the two rows of VWSs (inby and outby) as a function of face location, are shown in Figures 12 through 13. Figure 14 shows stress changes versus time for the VWSs which were not destroyed during the mining process.

1) The stress changes begin to increase rapidly when the face is roughly 150-200 ft behind (inby) the instrument locations, peak when the face reaches the instrumentation location, drop a little bit immediately after the face passes, and then increase again very slowly after the face is outby of the instrumentation location. This sequence of stress changes suggests that the stress drop after the face passes may be an "elastic drop" due to load decrease or plastic drop due to yielding of coal pillar or weak floor. The average rates of incremental stress changes during Phases I, II, and III are given in Table 1.

2) The peak value of the abutment pressure at the edge of the pillar is estimated as 2 to 3 times the premining vertical stress. This is based on the maximum observed stress change of about 620 psi which is approximately equal to the premining vertical stress, and an additional stress due to development of chain pillars.

Roof-Floor Convergence and Roof Sag

Roof-floor convergence as a function of time and face location for some of the convergence points are shown in Figures 15 and 16. Some of the 20 convergence points were destroyed by mining activities after they were installed.

The magnitude and rate of the convergence varies with the location of measurement. For example, the convergence values at point 3 and 4 in the crosscut are much greater than points 5 and 9 in the entry farthest from the panel. The average rates of convergence during Phases I, II and III are given below in Table 1. The normalized convergence as a function of normalized face location can be predicted using Eq. 1 for A=50 ft. Based on limited data available, roof sag is estimated as about 25 pct of the roof-floor convergence; and the remaining 75 pct is the floor heave.

Lateral Pillar Deformation

Lateral pillar deformation data along and across the panel and as a function of face position are shown in Figures 17 and 18. The deformation as a function of face position can be predicted by Eq. 1 by assigning A=0. The three-phase classification is also applicable to lateral pillar deformation and rates in the three phases are shown in Table 1.

Synthesis of data

Surface Subsidence, Convergence, Pillar Stress and Pillar Deformation as a Function of Face Position

A plot of different normalized variables above as a function of d/H are shown in Figure 19, and the rates for each variable in different Phases are given in Table 1.

Table 1 Length and Rate of Changes in the Three Phases for the Parameters

Parameters	Phase I		Phase II		Phase III		Units
	Range of d/H	Rate	Range of d/H	Rate	Range of d/H	Rate	
Subsidence	-0.5 to 0	2.6×10^{-3}	0 to 0.7	0.14	> 0.7	2.95×10^{-3}	in/ft
Pillar Deform.	< -0.14	2.08×10^{-5}	-0.14 to 0.19	5.38×10^{-4}	> 0.19	4.37×10^{-5}	in/ft
Pillar Stress	< -0.4	0.055	-0.4 to 0	0.95	> 0	Drop	psi/ft
Convergence	< -0.25	2.3×10^{-4}	-0.25 to -0.48	2.7×10^{-3}	> 0.48	6.25×10^{-4}	in/ft

Figure 19 indicates that stress changes in the pillar moves into Phase II when d/H is about -0.6. Surface subsidence enters Phase II when d/H=0. This shift is also reflected in moving from Phase II to Phase III for all these variables. There also appears to be a phase shift between occurrence of the peak incremental stress on pillars and peak convergence and lateral pillar deformation. This is probably because of the time-dependent deformation effects. The plots above can be used by the industry for planning additional supports in gate entries as well as planning land and structure use on the surface. An attempt will be made to plot similar data from other longwall faces in Illinois Coal Basin to develop unified plots for use by industry.

Subsidence Factor as a Function of Width to Depth Ratio

The data on width to depth ratio (W/H) and subsidence factor (S_{max}/m) for Illinois longwall coal mines, were compiled (Hood, 1981; Bauer and hunt, 1982; Mehnert et al., 1992 and Bureau of Mines, 1992) and plotted in Figure 20. Statistical analysis did not yield significant correlation between the subsidence factor and the W/H ratio. A slight increase in subsidence factor with increasing W/H ratio is indicated. The subsidence factor calculation is sensitive to time and the mining height. The data presented in Figure 20 may or may not have been calculated for the same time, and furthermore it may not have been calculated for the average mined-seam thickness below the subsidence line. These differences do not permit accurate analysis of data in Figure 20.

Concluding Remarks

This paper has presented preliminary results of an ongoing study to develop subsidence characteristics and data on in-mine ground movements. These results will be used to assess performance of the geometry of chain pillars. Alternative geometries for chain pillars will be developed and their performance simulated using SIU PANEL.3D and the laminated models. It is expected that these studies will lead to design of chain pillars in Illinois Basin coal mines.

Acknowledgement

The authors gratefully acknowledge the financial support of the Illinois Mine Subsidence Program funded by the Illinois Coal Development Board through the Illinois Department of Energy and Natural Resources, U. S. Bureau of Mines, the coal company and the College of Engineering at SIUC.

References

Bauer, R. A. and S. R. Hunt, "Profile, Strain, and Time Characteristics of Subsidence from Coal Mines in Illinois," Proc. Workshop on Surface Subsidence Due to Underground Mining, West Virginia University, Morgantown, WV, 1982, pp. 207-218.

Powell, L. R., Private Communication (Bureau of Mines), 1992.

Chugh, Y. P., Pytel, W. and Z. Yu, "Determination of Floor Bearing Capacity of Full Size Pillars and Size Reduction Factors by Instrumenting Longwall Chain Pillars", Final Report to Illinois Mine Subsidence Research Program, Illinois Geological Survey, September 1992.

Mark, C., "Pillar Design Methods for Longwall Mining", Information Circular 9247, Bureau of Mines, 1990.

Mehnert, B. B., Roosendaal, D. J. V. and R. B. Bauer, "Long-term Subsidence Monitoring Over a Longwall Coal Mines in Southern Illinois," Proc. Third Subsidence Workshop due to Underground Mining, West Virginia University, Morgantown, WV, 1992, pp. 311-316.

Newman, D. A., "In Situ Yield Behavior of Coal Pillar," International Journal of Mining and Geological Engineering, Vol. 7, 1989, pp. 163-170.

Peng, S. S. and H. S. Chiang, Longwall Mining, John Wiley & Sons, 1984.

Yu, Z., Karmis, M., Jarosz, A. and C. Haycocks, "Development of Damage Criteria for

Buildings Affected by Mining Subsidence," Proc. Sixth Annual Workshop Generic Mineral technology Center Mine Systems Design and Ground Control, Fairbanks, Alaska, 1988, pp. 83-92.

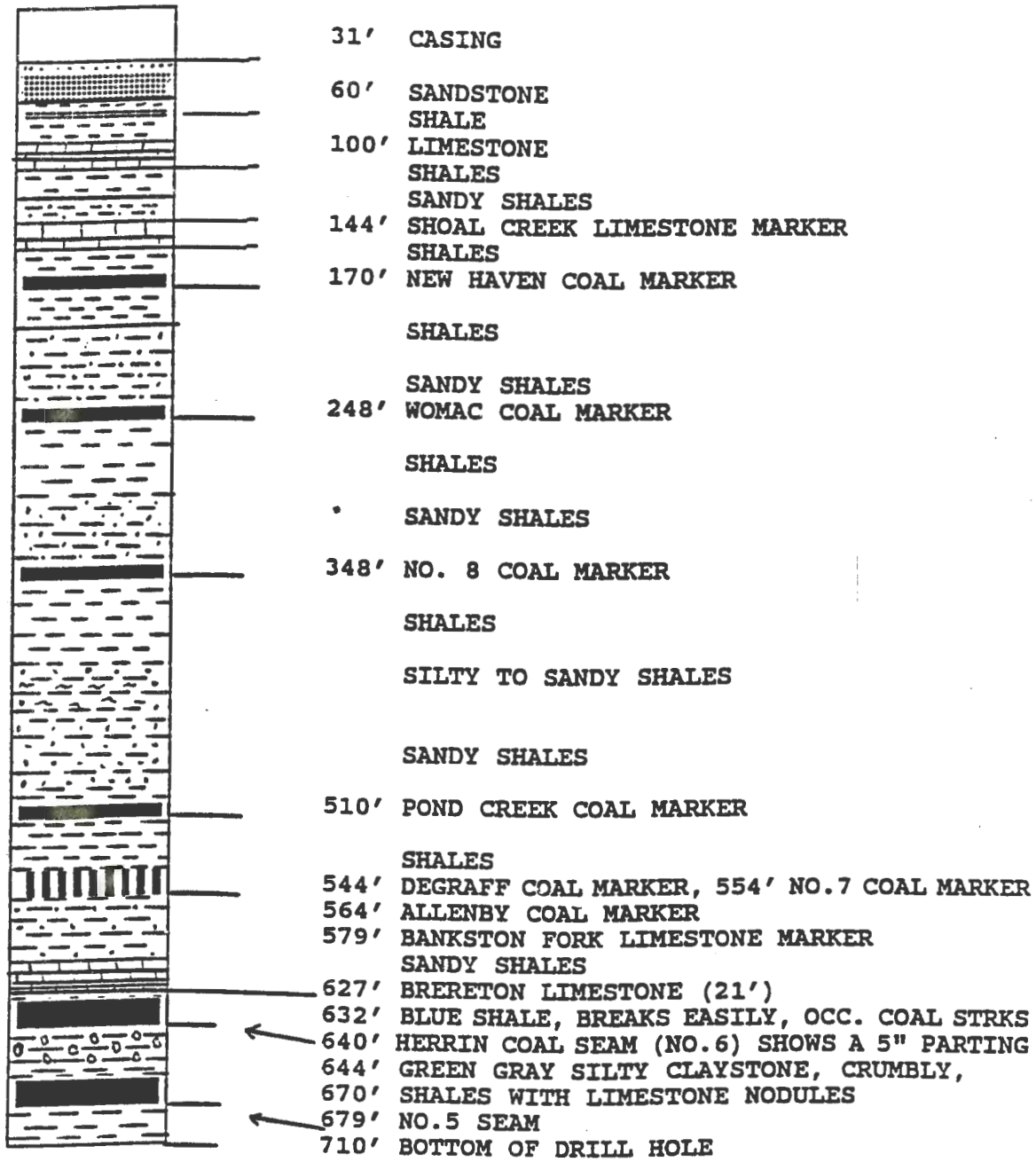

Figure 1. Lithologic log of the studied area. - -

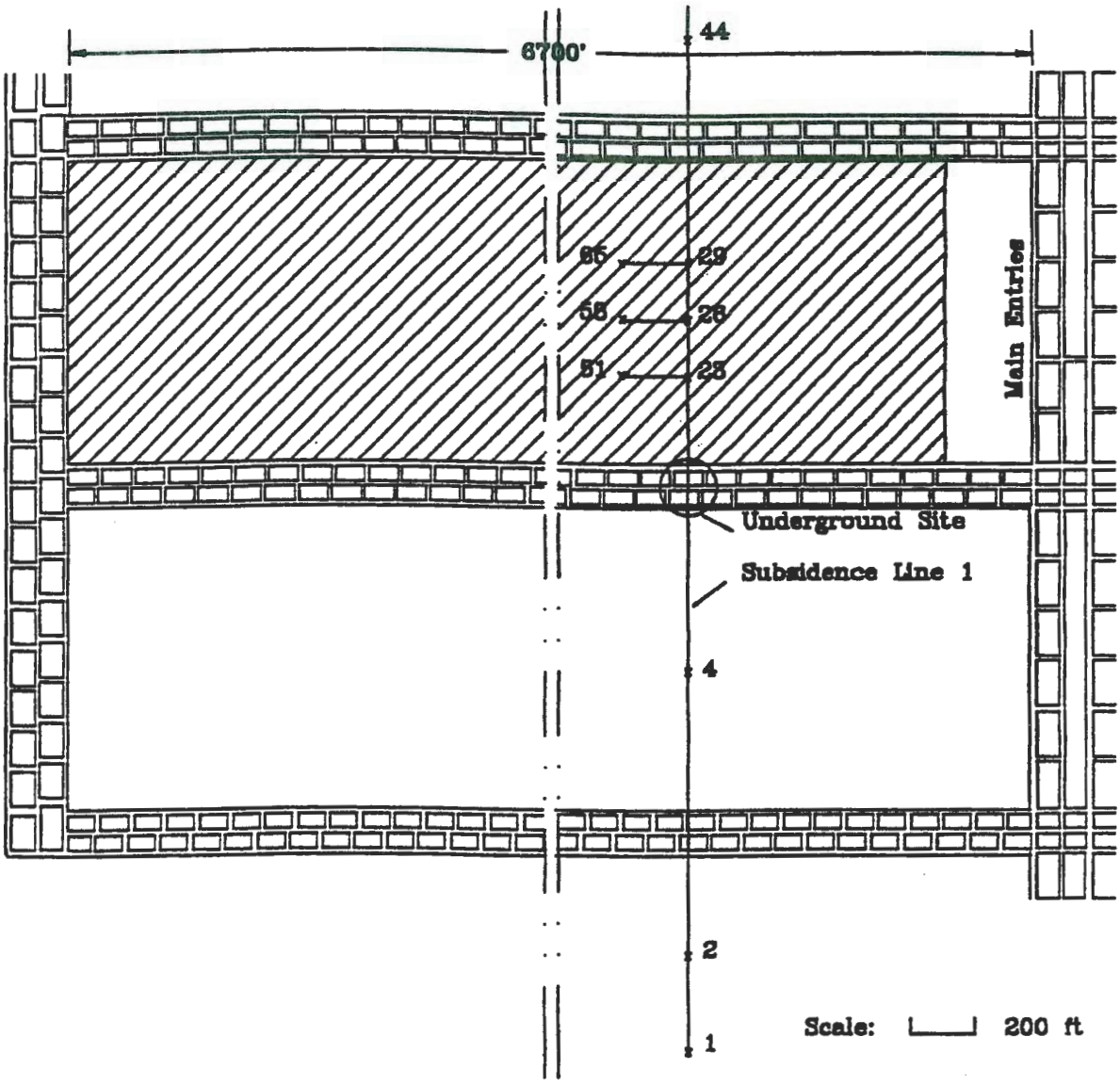

Figure 2. Panel layout and the location of the monitoring site.

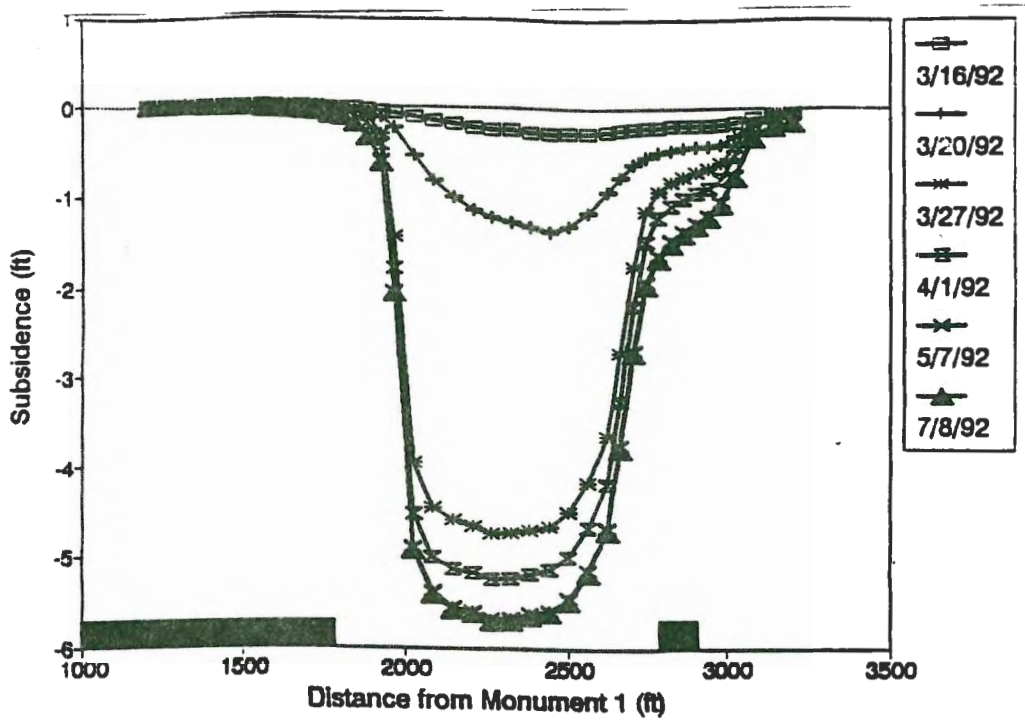

Figure 4. Subsidence across the panel.

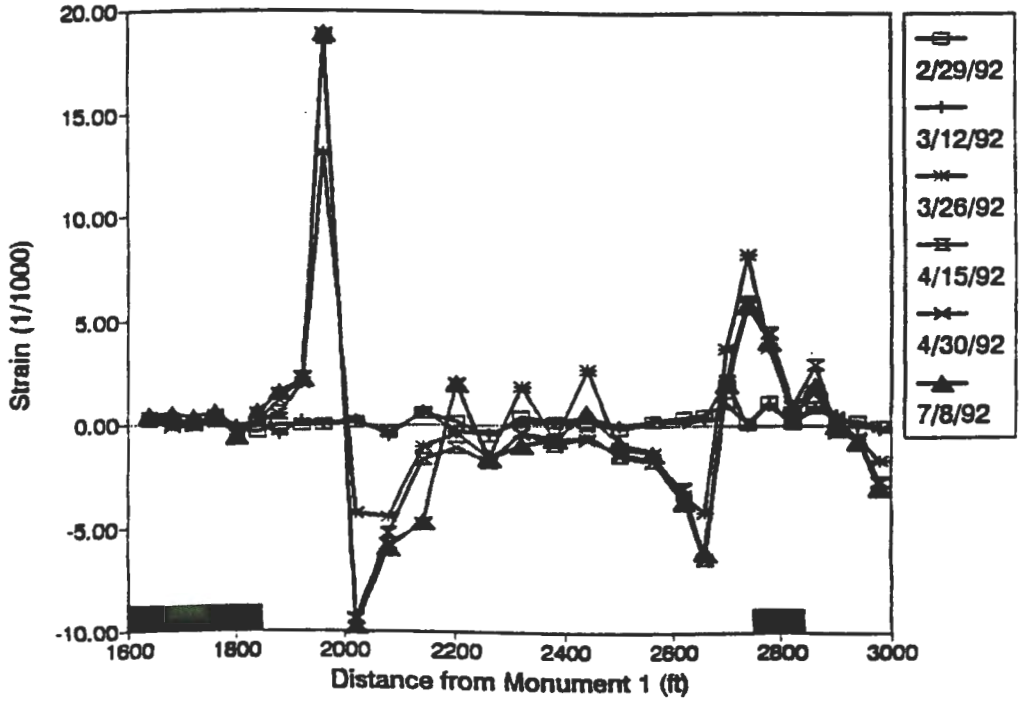

Figure 5. Horizontal strain across the panel.

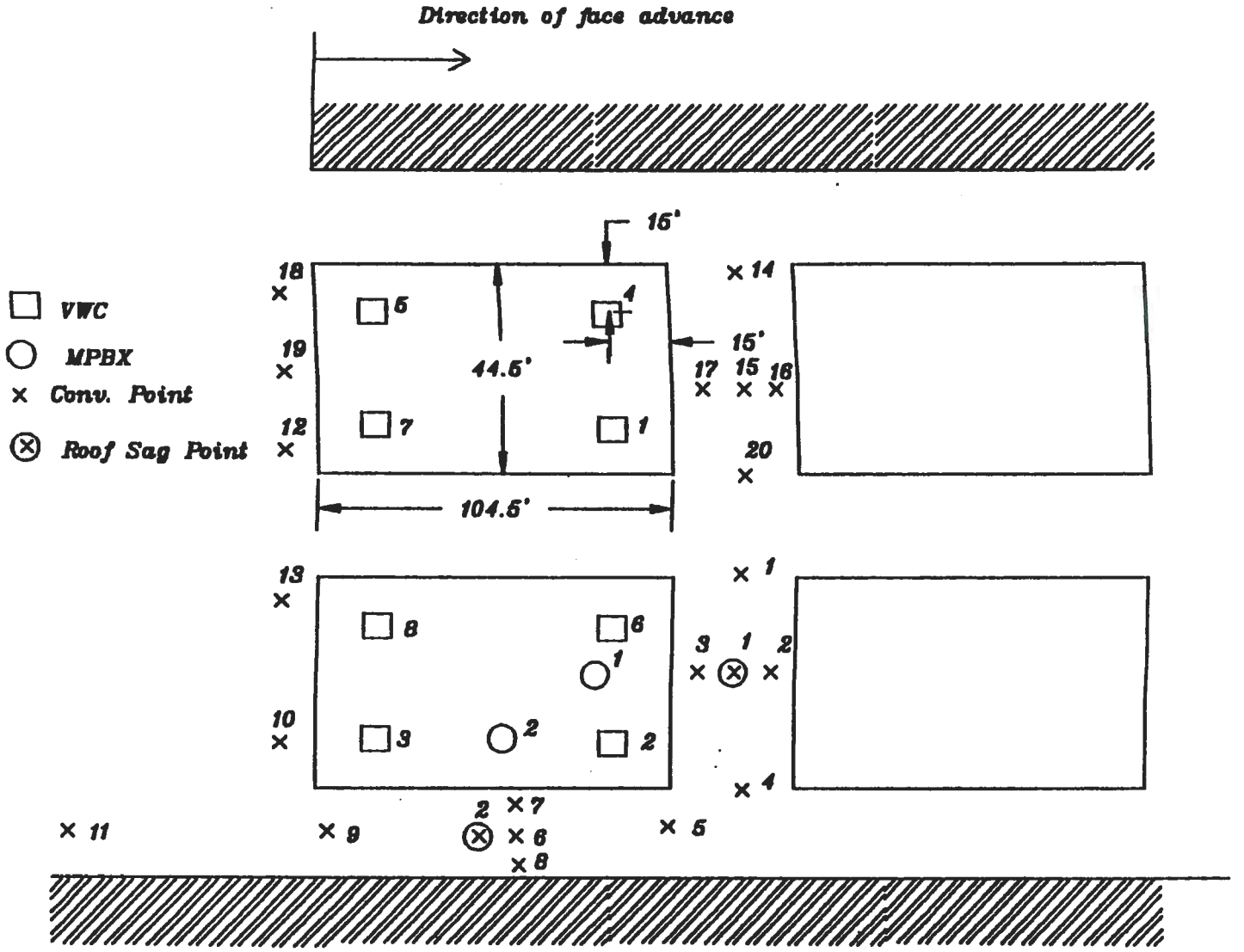

Figure 3. Layout of the underground instrumentation.

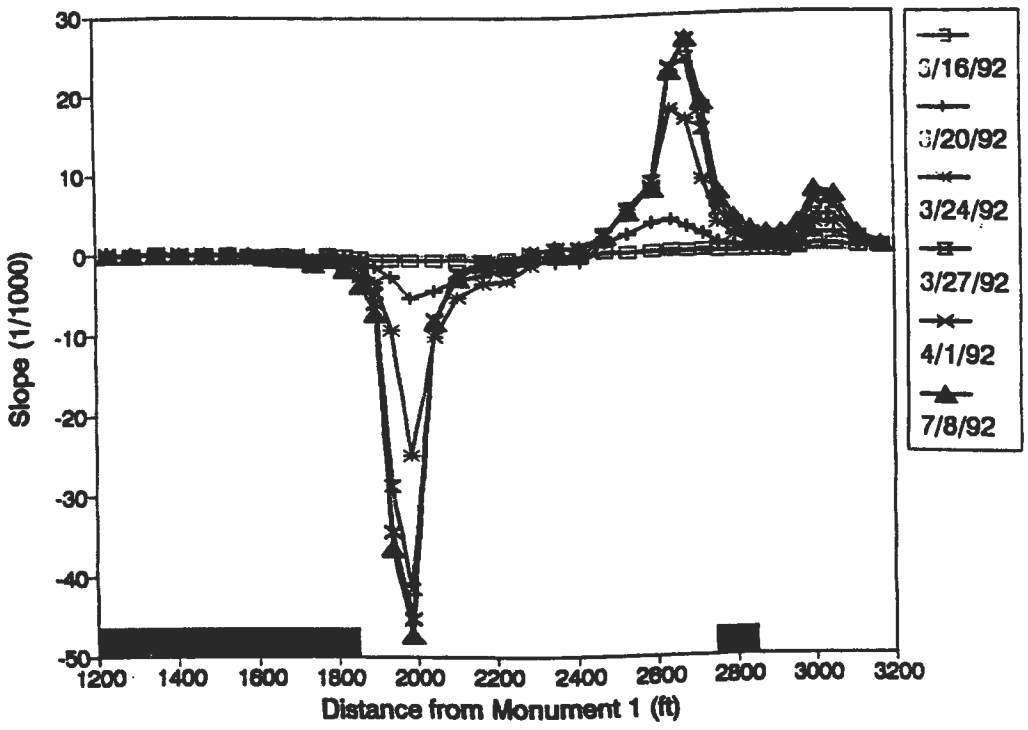

Figure 6. Slope across the panel.

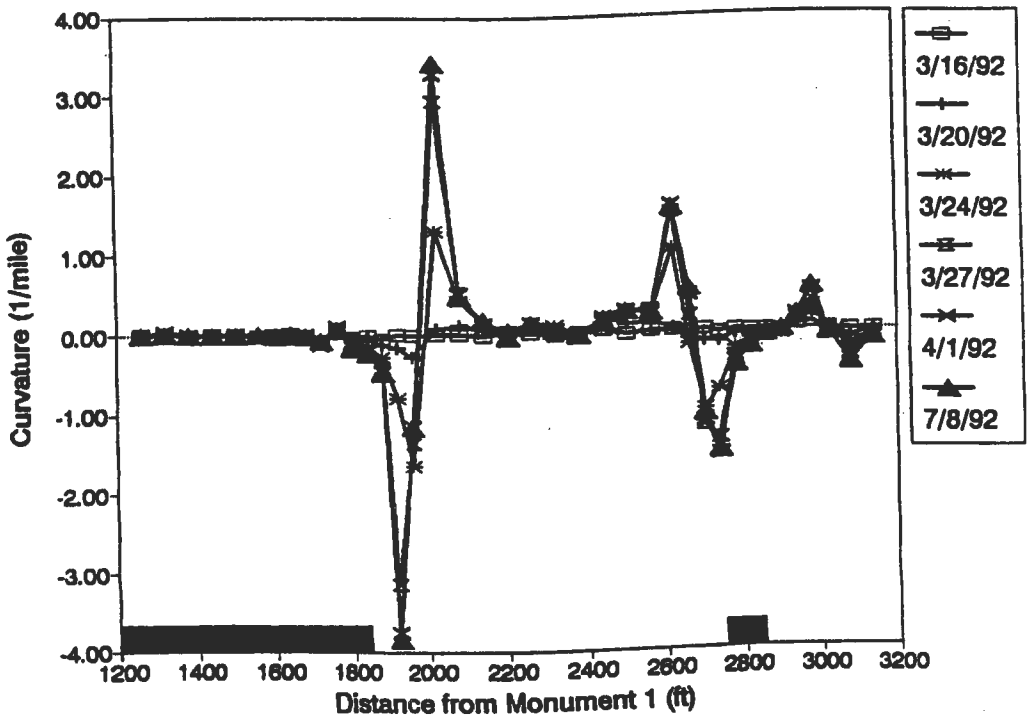

Figure 7. Curvature across the panel.

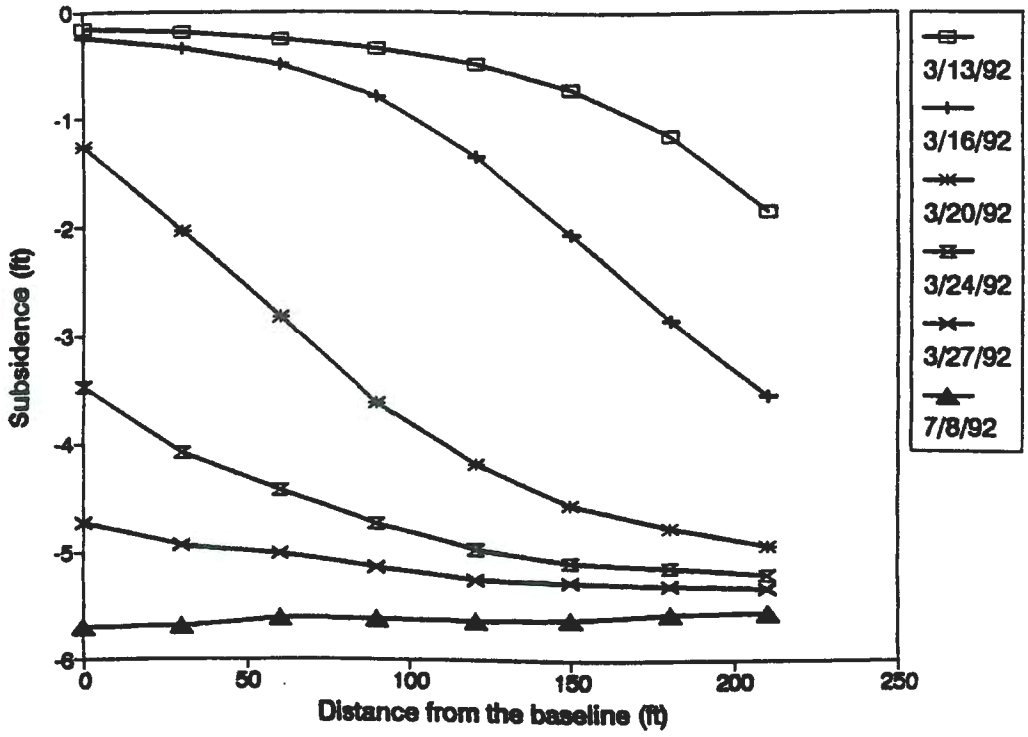

Figure 8. Subsidence along the panel.

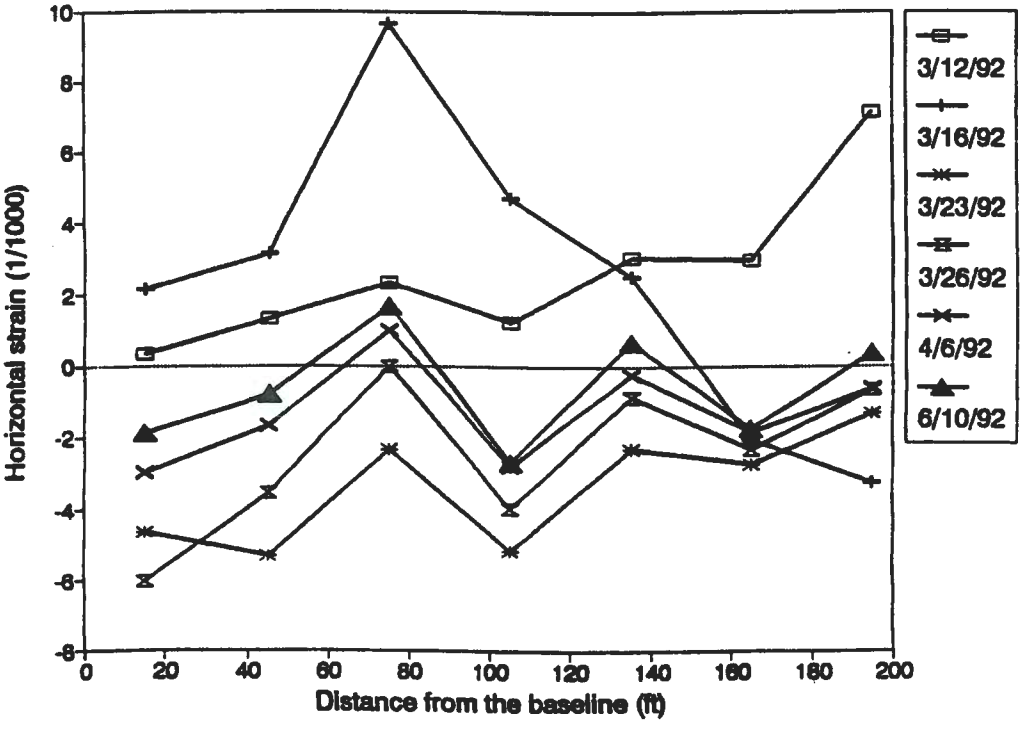

Figure 9. Horizontal strain along the panel.

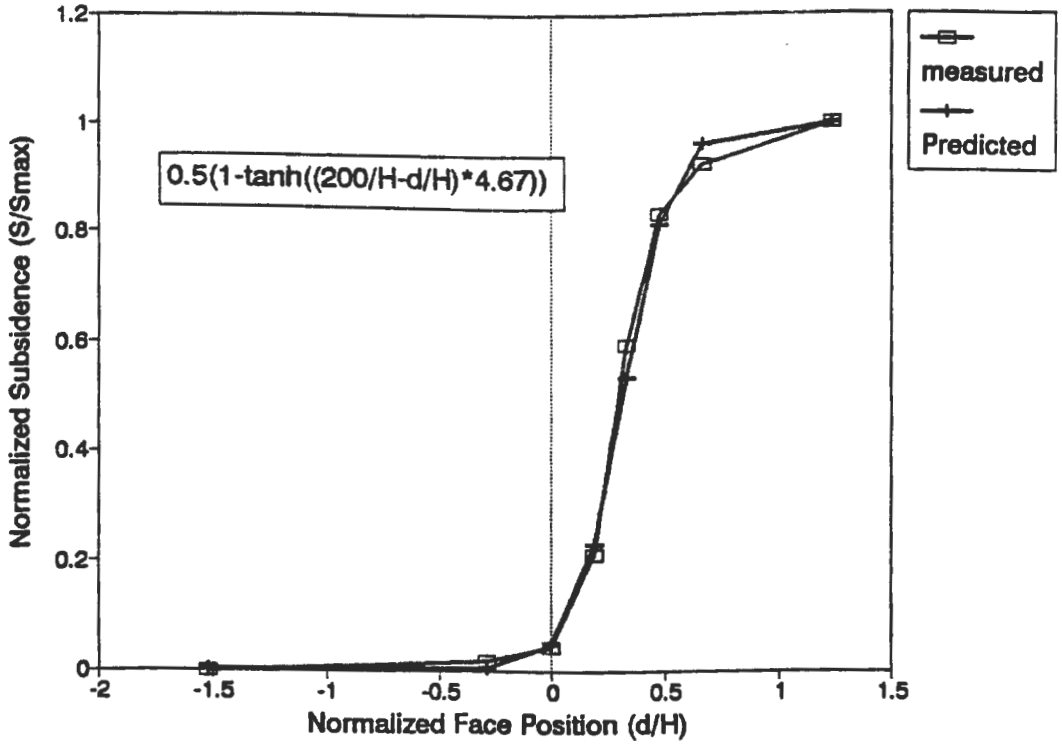

Figure 10. Subsidence as a function of face position.

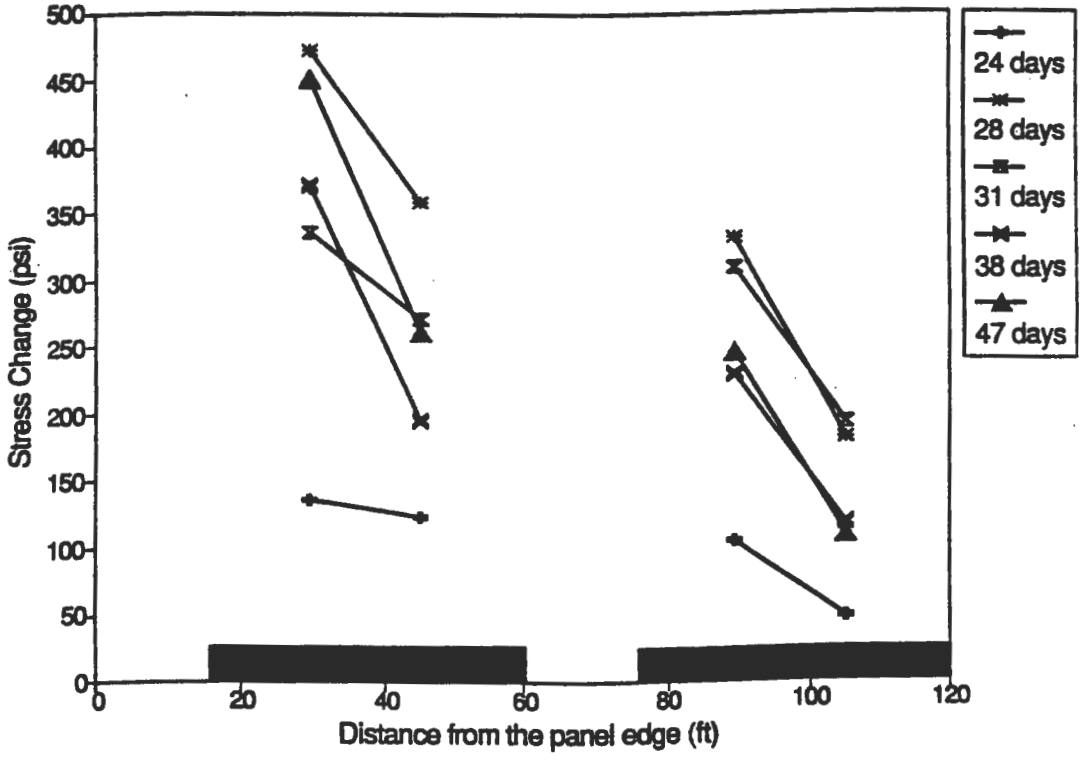

Figure 11. Distribution of stress-changes in the chain pillars along the transverse direction.

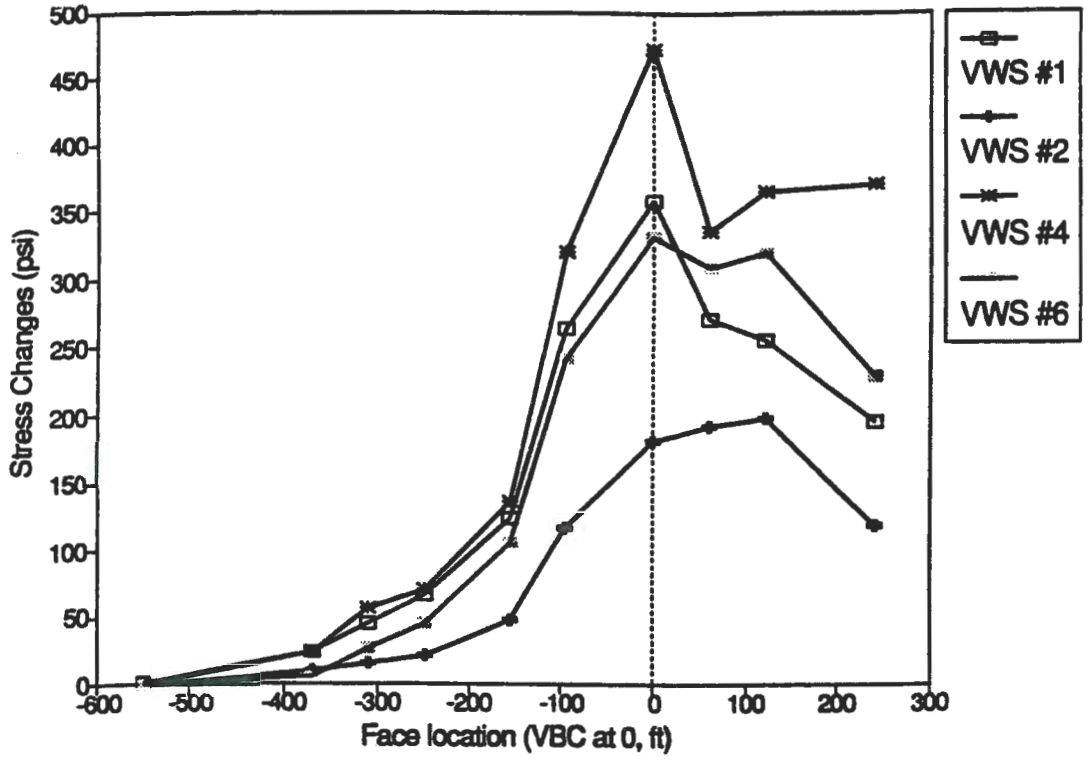

Figure 12. Pillar stress changes as a function of face position for the outby row of VWS.

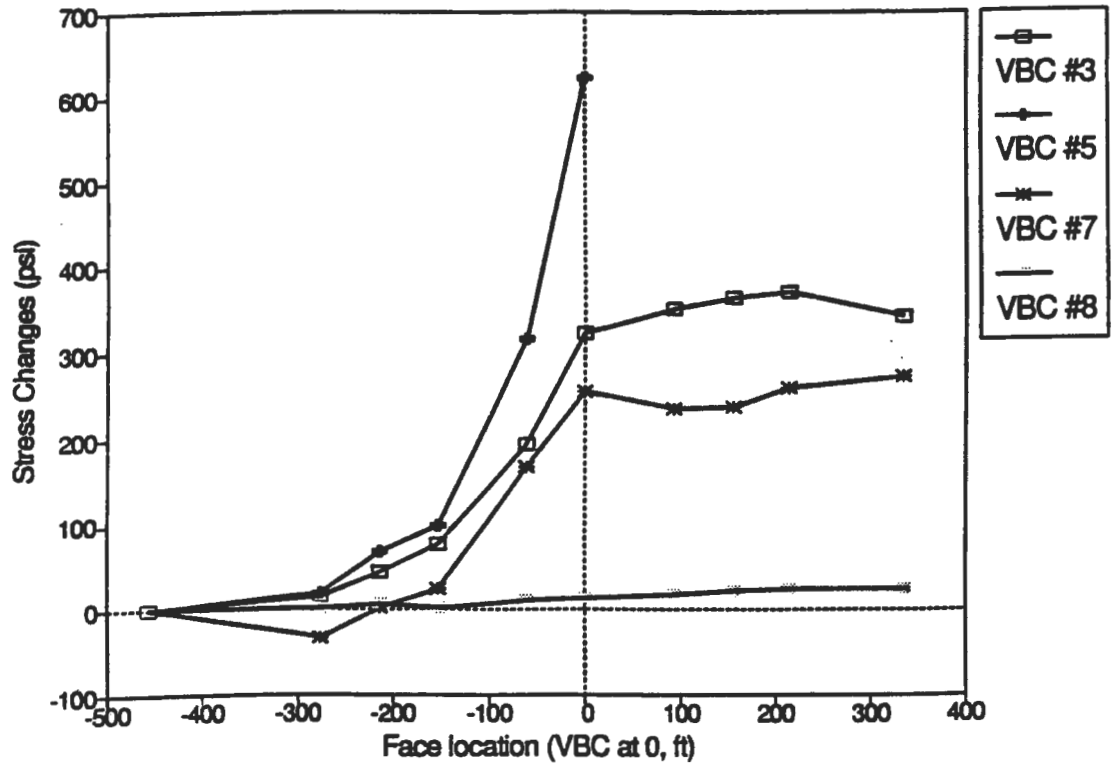

Figure 13. Pillar stress changes as a function of face position for the inby row of VWS.

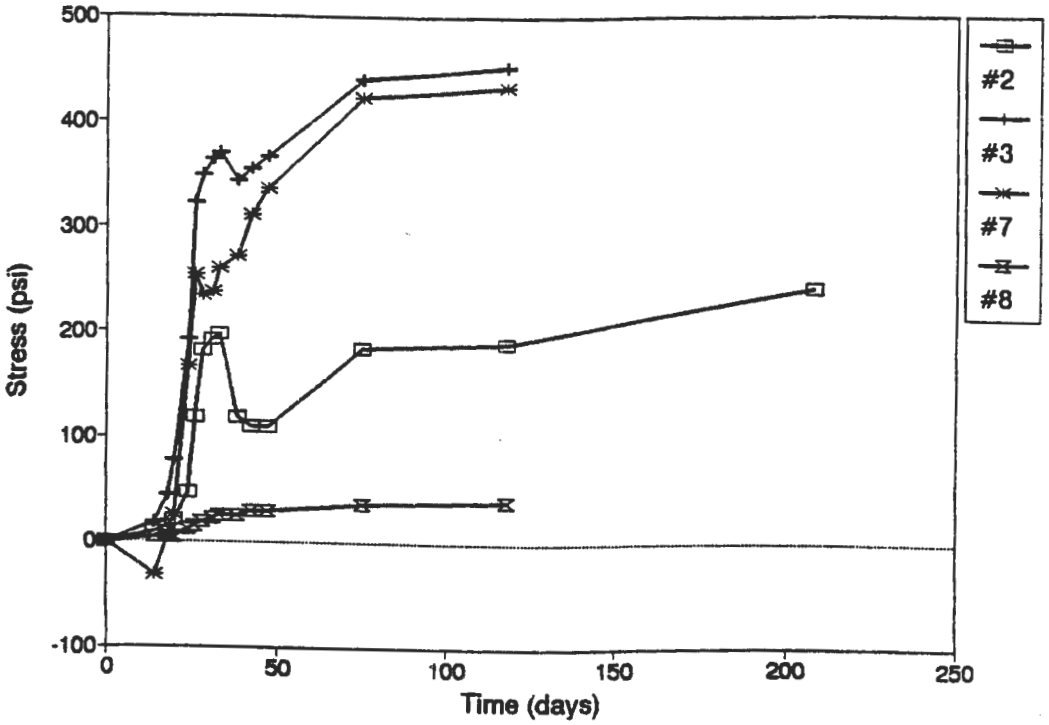

Figure 14. Pillar stress changes as a function of time.

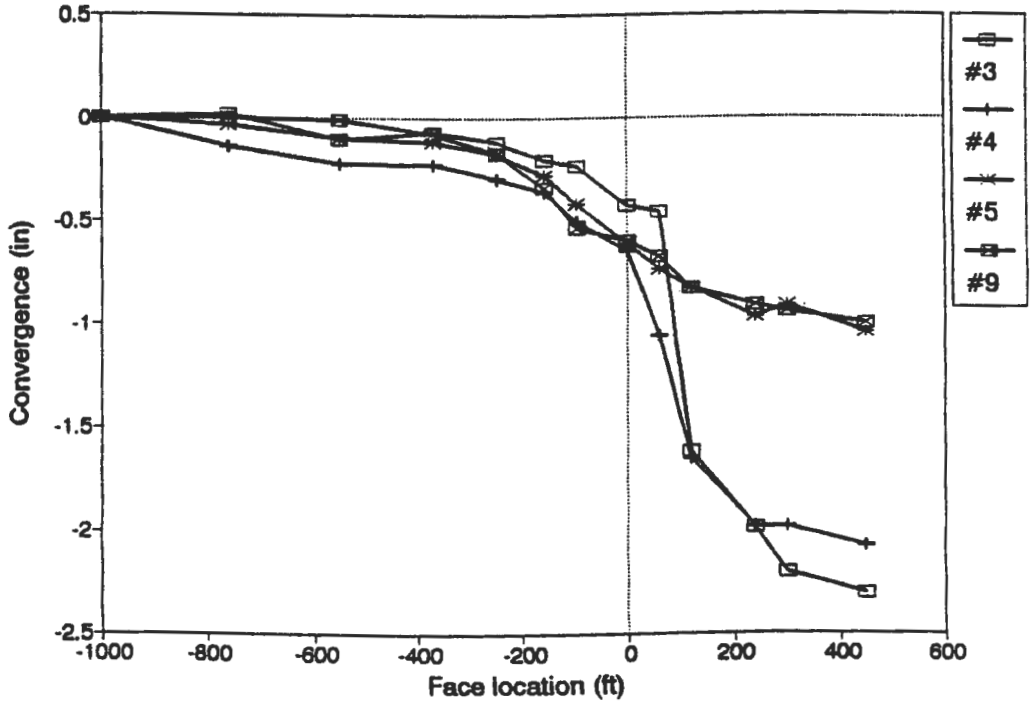

Figure 15. Convergence as a function of face position.

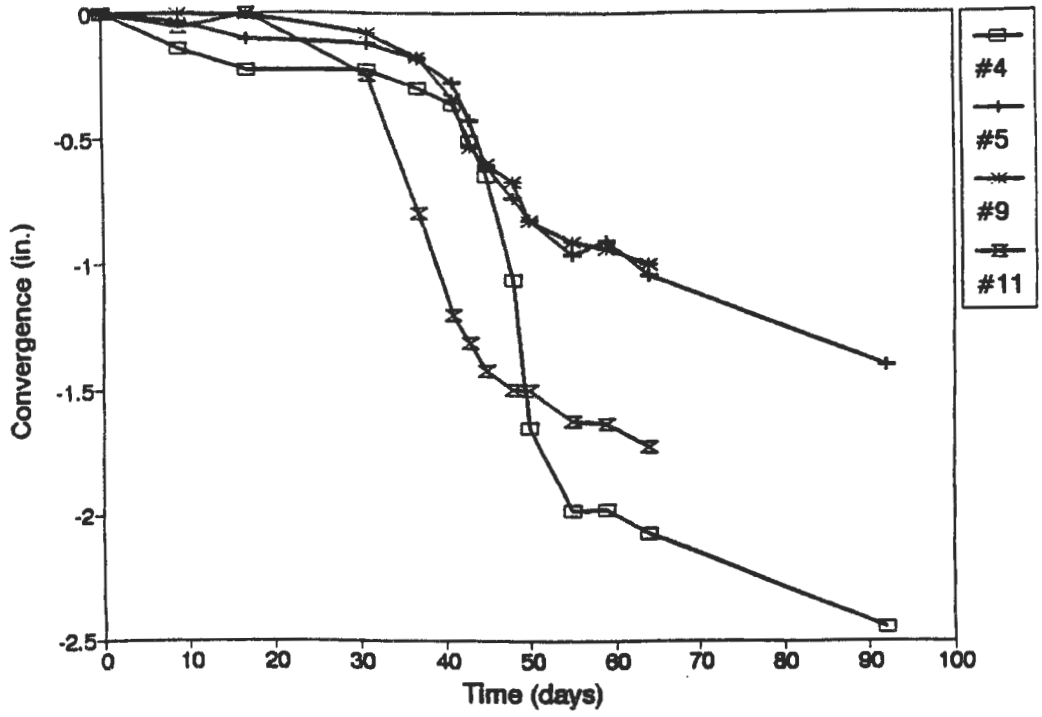

Figure 16. Convergence as a function of time.

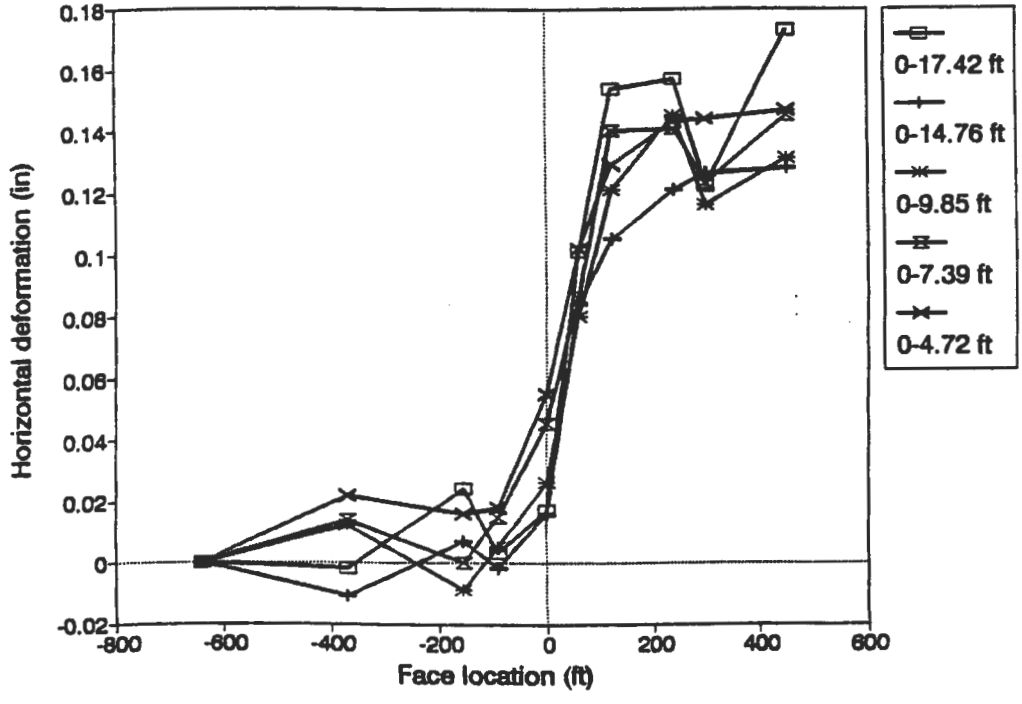

Figure 17. Lateral pillar deformation along the panel as a function of face position.

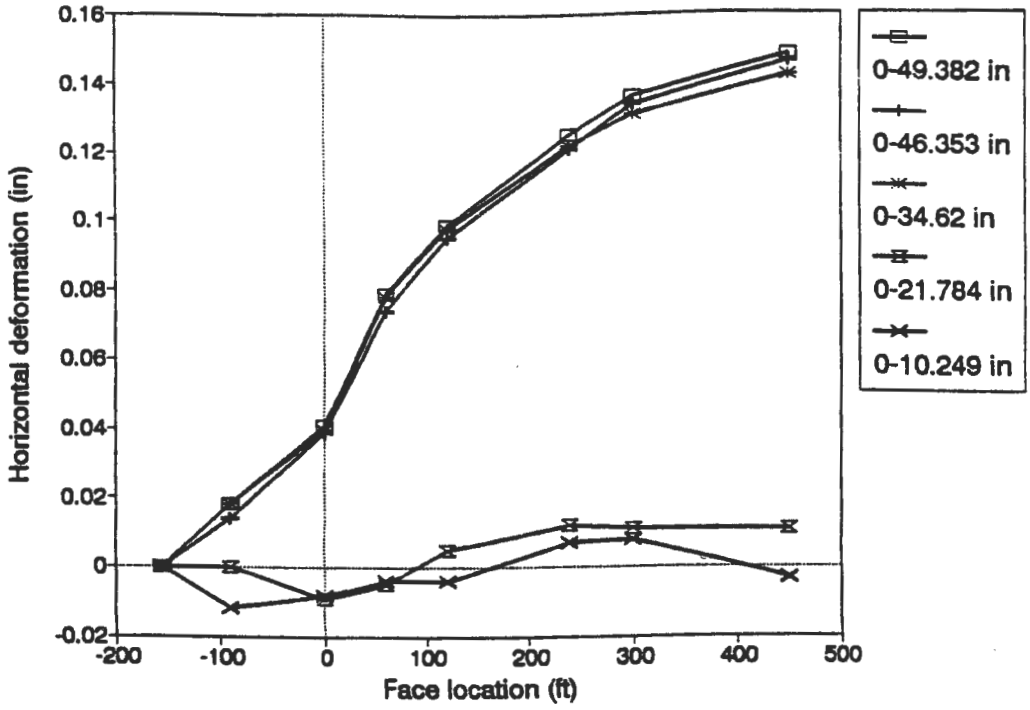

Figure 18. Lateral pillar deformation across the panel as a function of face position.

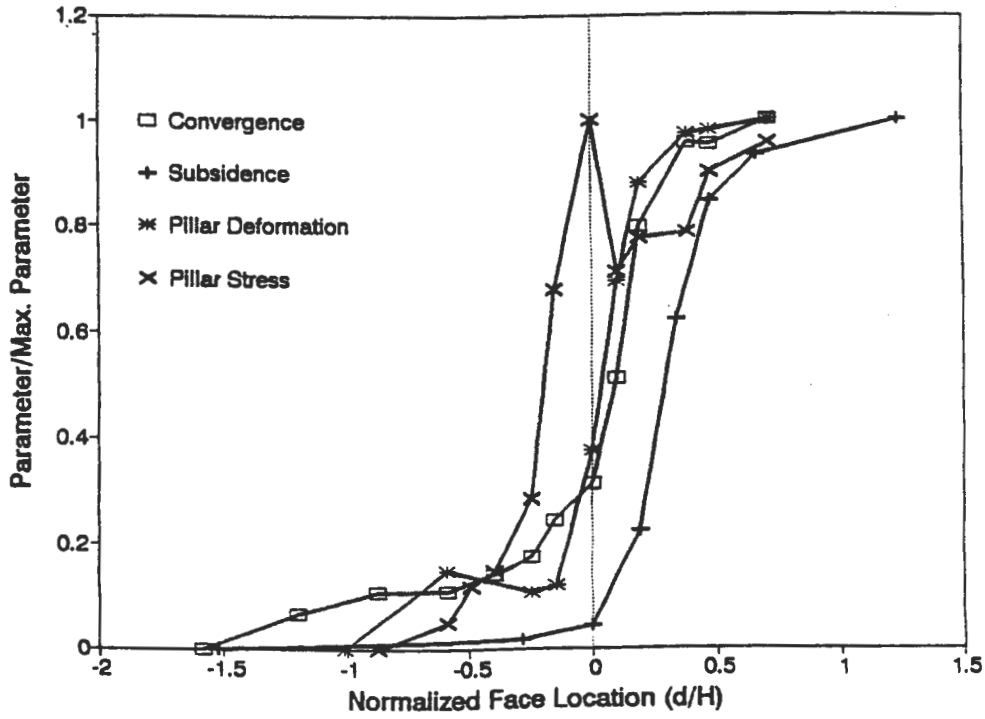

Figure 19. Various ground control parameters versus face position.

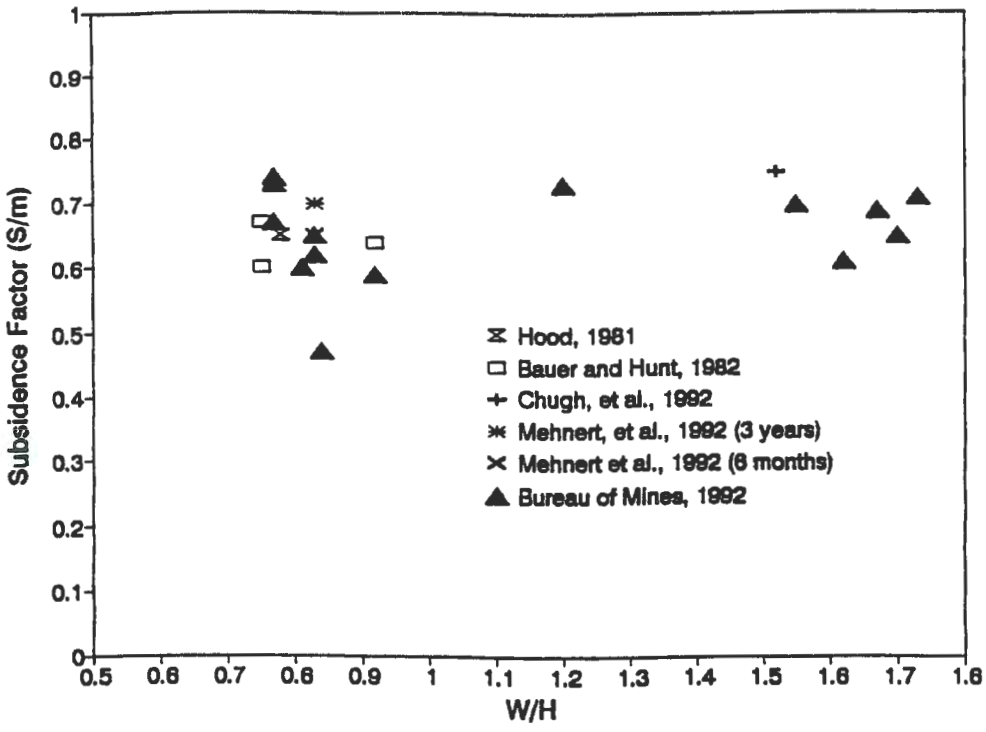

Figure 20. Subsidence factor versus W/H ratio.

Proceedings
Fourth Conference on Ground Control For Midwestern U.S. Coal Mines

held at

Ramada Hotel
Mt. Vernon, Illinois

November 2-4, 1992

Editors

Yoginder P. Chugh

and

Georgia Anne Beasley

Department of Mining Engineering
Southern Illinois University

SYMPOSIUM SPONSORED BY

Illinois Department of Energy and Natural Resources
SIUC Illinois Mining and Mineral Resources Research Institute
Illinois Mine Subsidence Research Program
SIUC Department of Mining Engineering
Southern Illinois University at Carbondale
U.S. Bureau of Mines

November, 1992